Trajectory Tracking of Optimal Social Distancing Strategies with Application to a CoVid-19 Scenario

Francesco Di Lauro[1], István Zoltan Kiss[1], Daniela Rus[2], Cosimo Della Santina[3]

***Abstract*— This letter proposes the use of nonlinear feedback control to produce robust and reactive social distancing policies that can be adapted in response to an epidemic outbreak. A trajectory tracking algorithm is proposed, and its effectiveness is analytically proven when acting on a low-dimensional approximation of the epidemics. Means of mapping the inputs and output of this controller to the real network dynamics of the pandemics are introduced. The strategy is tested with extensive simulations in a CoVid-19 inspired scenario, with particular focus on the case of Codogno - a small city in Northen Italy that has been among the most harshly hit by the pandemics. The proposed algorithm generates dramatic reductions of epidemic levels, while maintaining a total level of social distancing close to the nominal optimum.**

I. Introduction

Defining policies to control pandemics is a long-lasting research challenge, which has been recently invested by a new burst of interested due to Covid-19 outbreak. Until a vaccine is available, the most effective way [1], [2] of limiting the spread of a disease has proven to be restraining people from interacting at a close distance, from soft measures to full lockdown (referred as control policies hereinafter). At the same time, it is also widely accepted that extreme levels of lockdown are unsustainable in the long run, due to the vast range of pernicious secondary effects that they may provoke [3], [4]. Finding the right trade-off is clearly a matter involving politics and sociological arguments that we do not aim at addressing here. In this context, the role of science has been the one of providing a range of possible alternatives, and establish their effectiveness. Control theory has been soon identified as a possible tool for deriving such policies, as discussed in [5].

Usually, the evolution of epidemic curves is described by low dimensional compartmental models [6]. In turn, they can be adapted to act on network models [7] that take into account social structures. Arguably, indeed, a critical challenge in modeling epidemic spreading arises from the complexity of the social contact structure of the population experiencing the outbreak. Although complex, data-driven models of epidemics that include the high dimensional network-like structure of the problem are available [8], [9], developing controllers directly based on such models is a burdensome task, and results require extensive simulations of not immediate interpretation. Thus, most of the attention has been devoted to open loop optimal control applied on simpler models, to shed light on some important tasks. Examples are [10] selecting optimal timing when there are constraints on the length of the action, [11] solving a linear quadratic problem integrating number of deaths and economic effects, and [12] discussing the problem of optimal peak reduction.

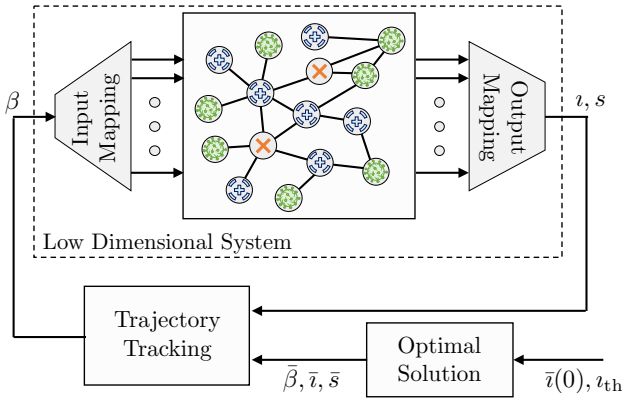

Fig. 1. Block diagram of the strategy proposed in this paper. Input and output maps are proposed matching outputs and inputs of a realistic network model of the pandemics, to a low dimensional compartmental model. A nonlinear feedback control action acts within this compact representation implementing trajectory tracking of an optimal control policy, which is designed to maintain $\imath < \imath_{\rm th}$ under nominal conditions.

However, open loop strategies have been shown to be quite prone to the many uncertainties affecting the controlled system - many of which arising from the difficulties in modeling the underlying network structure [12]–[14]. Looking at the problem through the lenses of control theory, it appears clear that these robustness issues call for the implementation of feedback actions. Linear feedback controllers are proposed in [15], [16]. In [17] the loop is closed by periodically re-planning the optimal action, in a model-predictive-control fashion. In [18] a similar strategy is proposed, and robustified by means of interval arithmetic. Finally, [19] introduces an open-loop fast switching strategy with duty cycle selected through a slow feedback of the total infects.

To the authors best knowledge, no work has been done to design a feedback control policy that can be directly applied to the high dimensional network-structured dynamics of the epidemics. In this work, we aim at making a very first step in this direction. We propose to design a control policy as a trajectory tracking problem, where the reference is devised by means of optimal control. The latter is built up on the request that, in nominal conditions, the social distancing level is the minimum necessary to assure that the healthcare system capacity is never overburdened. Feedback is used to enforce the robustness of this action, without spoiling its effectiveness. The stability of the proposed feedback controller

[1] Francesco Di Lauro and István Zoltan Kiss are with Department of Mathematics, School of Mathematical and Physical Sciences, University of Sussex, Falmer, Brighton BN1 9QH, UK. [2]Daniela Rus is with the MIT Computer Science and Artificial Intelligence Laboratory, Massachusetts Institute of Technology, Cambridge, MA, USA. [3]Cosimo Della Santina is with the Cognitive Robotics Department, Delft University of Technology, 2628 CD Delft, The Netherlands, and with the Institute of Robotics and Mechatronics, German Aerospace Center (DLR), Oberpfaffenhofen, Germany. Contacts cosimodellasantina@gmail.com.

is discussed analytically when applied on a compartmental model. We then introduce a method based on arguments widely accepted in epidemics, which interfaces the low dimensional controller with the full network. We perform extensive simulations under realistic conditions, proving the effectiveness of the control architecture across a vast range of models.

To succinctly summarise, our work contributes with

- a feedforward action expressed in closed form which optimally flatters the infects curve,
- a provable trajectory tracking controller,
- two simple but effective strategies to interface the controller with a realistic network system,
- extensive simulations showing the effectiveness of the proposed reactive policy in a vast range of network simulations.

II. Background: Model of the Epidemics with Dynamic Interventions

Consider a fixed population of N individuals, and a disease spreading among them, through direct contacts. Each individual can be in either of three states: (i) susceptible, meaning that they can be infected by the pathogen; (ii) infected, meaning that they contracted the pathogen and they can now infect other people; (iii) recovered, which includes also dead subjects. We denote with $S(t), I(t), R(t)$ the number of people at time t who are susceptible, infected or recovered, respectively. We have that $S(t)+I(t)+R(t) = N$. We can therefore neglect the study of R, as its value can always be recovered from S, I and N. If the population is well mixed[1] the evolution of the disease can be well described by the so-called SIR model [6]

$$\dot{s}(t) = -\beta \imath(t) s(t), \quad i(t) = +\beta \imath(t) s(t) - \gamma \imath(t), \quad (1)$$

where $s(t)$ and $\imath(t)$ are the system state, indicating respectively the number of susceptible $S(t)$ and infectious $I(t)$, divided by the total population N. Without loss of generality, we will consider in the following $t = 0$ as the time in which $s + \imath = 1$, meaning that no subject is yet recovered from the disease. The constant γ and defines a transition rate from the pool of infected subjects, to the recovered ones. The product $\imath(t)s(t)$ captures the chances that a healthy person gets in contact with an infected one, and β is a scaling factor which reflects how infectious is the disease and how frequent is the close interaction between people. When social distancing policies are imposed, the value of β changes from a maximum of $\beta_{\max}$ (no policy put into place), to a minimum of 0 (total lock down). Therefore β is the control input of (1).

III. Control Strategy

We propose here a control strategy acting on system (1). As shown by Fig. 1, this architecture is made of two components: (i) an optimal open loop action, and (ii) a feedback controller implementing trajectory tracking. The first block takes as input the the maximum capacity of intensive care units in the local hospitals $\imath_{\text{th}}$ and an initial condition $\imath(0)$, and it generates as output a curve which is flattened enough to reach the threshold at its peak. The second block is a nonlinear feedback controller which robustly tracks this reference while minimally relying on model cancellations.

[1]This means that there are not well identifiable clusters of people, and the social interconnections are homogeneous. Note that we are not imposing this condition on our network simulation, in Secs. IV and V.

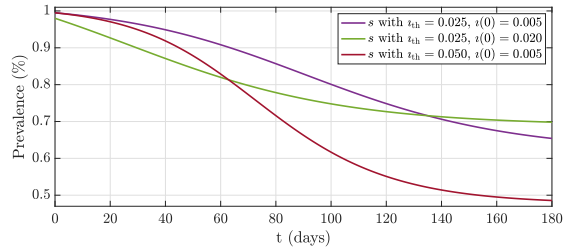

(a) Susceptible s

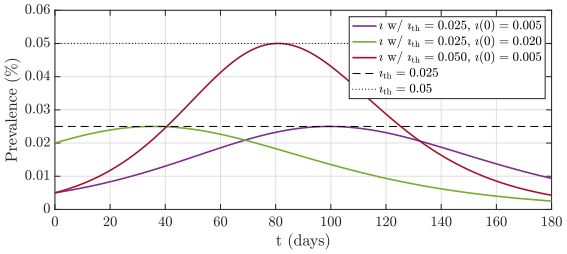

(b) Infected $\imath$

Fig. 2. Three examples of optimal evolutions resulting from (3), for different representative choices of $\imath(0)$ and $\imath_{\text{th}}$. The corresponding values of β are $0.1385/\text{days}$, $0.025/\text{days}$, and $0.1562/\text{days}$ respectively.

A. Optimal curve flattening under nominal conditions

Our aim here is to introduce a nominal strategy ("Optimal Solution" in Fig. 1) for optimally flattering the infection curve, so to keep the number of infected people $\imath$ within the maximum capacity of the health-care system, that we call $\imath_{th} > 0$. Enforcing this constraint is very important since exceeding it may provoke a critical failure of the health system, leading to a substantial increase of the total deaths not only from the pandemics but also from uncorrelated health issues. On the other hand, we want to keep the level of restriction on the population as low as possible, to tame possible secondary negative effects (see the Introduction for more details). We are interested in the case of a constant β - which however will become later variable by the action of the feedback controller. This is a simplification instrumental to make the optimal control problem more manageable. Although it is beyond the scope of this paper to relax this assumption, it is worth noticing that minimal changes are required in the case of piece-wise constant β, as all the arguments made here hold naturally.

We summarize the above considerations through the optimization problem

$$\max_{\beta \in \mathbb{R}} \ \beta, \quad \text{s.t. } 0 < \imath(t) \leq \imath_{\text{th}} \ \ \forall t \ \text{ and } \ (1). \quad (2)$$

We now propose a Lemma introducing a general solution to this optimal control problem.

Lemma 1. *The solution of* (2) *exists in closed form, and it is equal to*

$$\beta = -\frac{\gamma}{1-\imath_{\text{th}}} W_{-1}\left(-\frac{1}{e}\frac{1-\imath_{\text{th}}}{1-\imath(0)}\right), \quad (3)$$

where W_{-1} is the branch -1 of the Lambert W function [20].

Proof. Since the cost function is linear in the optimization parameter, the optimal value is to be found on the boundary of the feasible set. We want to set β in such a way that $\max_t \imath(t) = \imath_{th}$.

The maximum value of $\imath$ should be such that $i(t) = 0$. Combining this condition with the second equation in (1) yields $s^+ = \gamma/\beta$. Further, we can combine the first two lines of (1) into $\mathrm{d}\imath/\mathrm{d}s = \gamma/(\beta s) - 1$. This nonlinear ordinary differential equation can be solved together with the initial condition $s(0) = 1 - \imath(0), \imath(0)$, to get

$$\imath(s) = \frac{\gamma}{\beta} \ln\left(\frac{s}{1-\imath(0)}\right) - s + 1. \tag{4}$$

By inverting $\imath(s^+)$ for β, we get the desired optimal value such that $\max_t \imath(t) = \imath_{th}$. The following is a solution for all integer values of i.

$$\beta = -\frac{\gamma}{1-\imath_{\mathrm{th}}} W_i\left(-\frac{1}{e}\frac{1-\imath_{\mathrm{th}}}{1-\imath(0)}\right). \tag{5}$$

However, only W_{-1}, W_0 have values in the real line [20]. Moreover, it is always the case that $W_0 > W_{-1}$, which in turn assures that the larger value of β among the two possible solutions is always reached for $i = -1$, concluding the proof.

□

It is worth noting that the argument of W_{-1} is always between $-1/e$ and 0 since $0\ \imath(0) \leq \imath_{\mathrm{th}}$. This is exactly the range of arguments for which the -1 branch of the Lambert function is well defined [20]. Fig. 2 shows few instances of solutions for different values of $\imath(0)$ and $\imath_{\mathrm{th}}$. Note that the corresponding evaluation of the state (which we will call $\bar{\beta}, \bar{\imath}, \bar{s}$ hereinafter) can be obtained either by direct integration of (1) or by using the approximated closed form solutions, as for example in [21].

B. Trajectory tracking controller

The following Lemma introduces the tracking controller ("Trajectory Tracking" in Fig. 1) implementing the reactive regulation of the social distancing level β. Note that - although we consider here its use in conjunction with the optimal strategy introduced in the previous section - this controller is agnostic to the choice of the reference to be tracked, and as such is introduced.

Lemma 2. *The feedback loop composed by the control action*

$$\beta(s, \imath) = \psi_{\mathrm{i}}(\imath - \bar{\imath}) + \psi_{\mathrm{s}}(s - \bar{s}) + \bar{\beta}\left(\frac{\bar{s}\bar{\imath}}{s\imath}\right) \tag{6}$$

and the SIR model (1)*, is such that*

$$\lim_{t\to\infty}(s, \imath) = (\bar{s}, \bar{\imath}), \tag{7}$$

for all $s, \imath, \psi_{\mathrm{i}}, \psi_{\mathrm{s}} > 0$, if $\bar{s}, \bar{\imath}, \bar{\beta}$ is a solution of (1)*.*

Proof. Consider the linear change of coordinates

$$x = -\frac{1}{\gamma}(\imath + s). \tag{8}$$

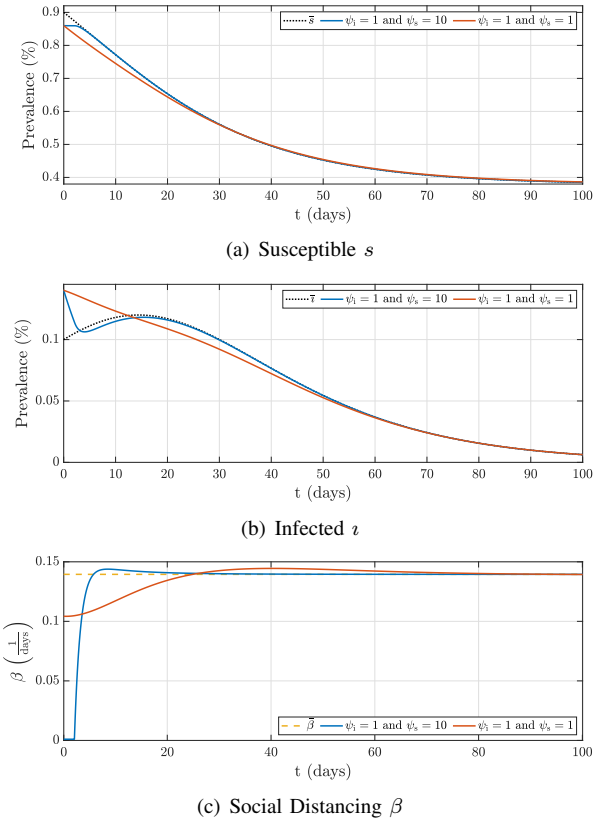

(a) Susceptible s

(b) Infected $\imath$

(c) Social Distancing β

Fig. 3. Two executions of the proposed control architecture when applied to system (1). Two different choices of control gains are considered. The other parameters are $\gamma = 0.1$, $\beta_{\max} = 0.22$, $\bar{\imath}(0) = 0.1$, $\imath_{\mathrm{th}} = 0.12$, $\imath(0) = 0.14$.

Adding up the two equations in (1), yields $i + \dot{s} = -\gamma\imath$. We can therefore establish the inverse change of coordinates

$$\imath = \dot{x}, \quad s = -\gamma x - \dot{x}. \tag{9}$$

Combining the latter, with the second equations in (1) allows writing the following equivalent formulation of the SIR dynamics

$$\ddot{x} = -(\gamma x + \dot{x})\dot{x}\beta - \gamma\dot{x}, \tag{10}$$

which is in normal form.

We take the following control action

$$\beta(x, \dot{x}) = -\frac{\gamma\dot{\bar{x}} + \ddot{\bar{x}}}{(\gamma x + \dot{x})\dot{x}} + \alpha_{\mathrm{p}}(\bar{x} - x) + \alpha_{\mathrm{d}}(\dot{\bar{x}} - \dot{x}), \tag{11}$$

with $\alpha_{\mathrm{p}} > \gamma\alpha_{\mathrm{d}} \geq 0$ being the gains of the PD-like action. This produces the closed loop dynamics

$$\ddot{e} = (\gamma + \alpha_{\mathrm{d}}(\gamma x + \dot{x})\dot{x})\dot{e} + \alpha_{\mathrm{p}}(\gamma x + \dot{x})\dot{x}e, \tag{12}$$

where $e = \bar{x} - x$. By hypothesis $\gamma + \alpha_{\mathrm{d}}(\gamma x + \dot{x})\dot{x} > 0$ and $\alpha_{\mathrm{p}}(\gamma x + \dot{x})\dot{x} > 0$. Therefore, both e and $\dot{e}$ converge exponentially to zero (see for example [22]), which combined with (9) yields (7).

Concluding the proof requires showing the equivalence of (11) and (6). Substituting the references $\ddot{\bar{x}}$ calculated from (10) into (11) yields $\gamma\dot{\bar{x}} + \ddot{\bar{x}} = (\gamma\bar{x} + \dot{\bar{x}})\dot{\bar{x}}$. Eq. (10) is obtained by considering that $\dot{x} = \imath$ and (8), and by taking $\psi_{\mathrm{i}} = \alpha_{\mathrm{p}}/\gamma - \alpha_{\mathrm{d}}$ and $\psi_{\mathrm{s}} = \alpha_{\mathrm{p}}/\gamma$. Note that the latter are always strctily positive by construction.

□

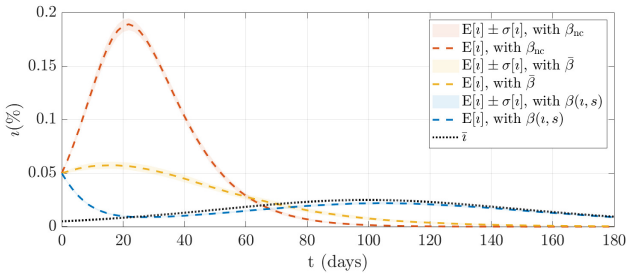

(a) Uncontrolled, open loop, and scenario (i)

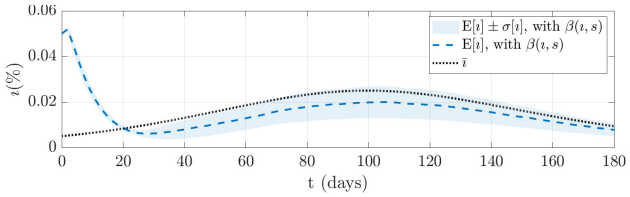

(b) Scenario (ii)

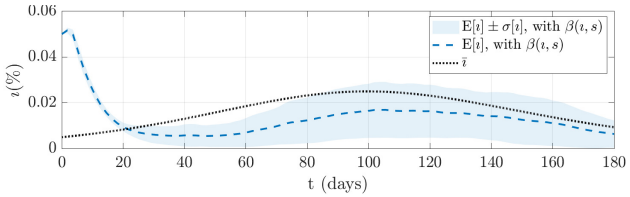

(c) Scenario (iii)

Fig. 4. Percentages of infected subjects of the Codogno case of study. In Panel (a) uncontrolled, open loop, and scenario (i) closed loop performances are reported, together with their one σ (standard deviation) band. Panel (b) and (c) show the closed loop performance for scenario (ii) and (iii) respectively.

We want our control action to remain limited when acting on a neighborhood of $s\imath = 0$. Also, it is not meaningful to act on the system by changing β to negative values. Similarly, it is not acceptable to get β greater than

$$\beta(s,\imath) = \left[\psi_{\mathrm{i}}(\imath - \bar{\imath}) + \psi_{\mathrm{s}}(s - \bar{s}) + \bar{\beta}\left(\frac{\bar{s}\bar{\imath}}{[s\imath]_{\epsilon}^{\infty}}\right)\right]_{0}^{\beta_{\max}}, \qquad (13)$$

where $\epsilon > 0$ is a small constant, and $[a]_l^u$ is is equal to l or u if $a < l$ or $a > r$ respectively, and equal to a otherwise. Fig. 3 reports two examples of application of the algorithm to the SIR model (1).

IV. Network Control

A. Network Model

Two fundamental aspects that we want to include in our refined model are (i) people interact through heterogeneous contact structures, i.e. the population is not well-mixed, (ii) real epidemics have an intrinsic degree of stochasticity, therefore they cannot be exactly described by ODEs systems such as (1). The epidemics on networks paradigm [7] allows us to include both phenomena: the contact structure is modeled by a network, in which individuals are modeled as nodes interacting only with their neighbours through links. Links carry the disease from infected nodes to their susceptible neighbours at a constant rate β_{n}. Infected nodes recover independently at a constant rate γ, after which they do not participate further to the epidemic. Initialization of the epidemic is made by turning $I(0) = N\imath(0)$ randomly

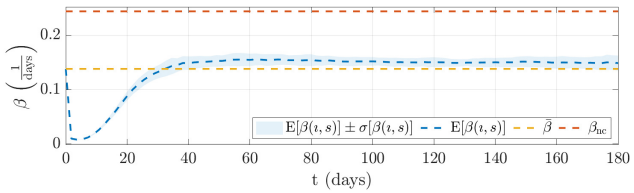

(a) Scenario (i)

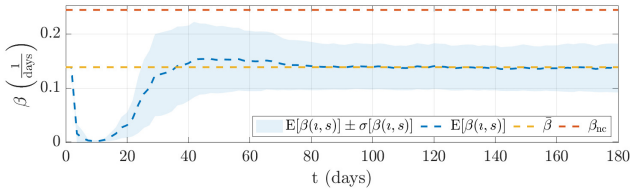

(b) Scenario (ii)

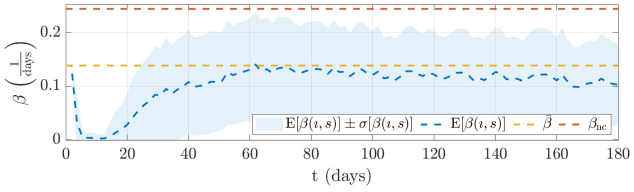

(c) Scenario (iii)

Fig. 5. Level of social distancing (0 is high and $\beta_{\max}$ is low) of the Codogno case of study. The closed loop performances for the three scenarios are reported, together with their one σ (standard deviation) band. The nominal reference $\bar{\beta}$ and the value corresponding to no social distancing $\beta_{\max}$ are also shown for comparison.

chosen nodes to the infectious status at time 0. The others are susceptible. The resulting process is modelled as a continuous time Markov chain, with a state space of dimension 3^N. In this paper, we make use of the Gillespie algorithm [23] adapted to networks (see [7, Appendix]) to do extensive simulations on different instances of Erdős-Rényi networks [24]. The main idea can be concisely described as follows: start with N isolated nodes, then, for each pair of different nodes, a link connecting them is placed with probability $0 < p < 1$, with no multi-edges allowed. Hence, the probability of a node of having k neighbours follows a binomial distribution $\mathcal{B}(N-1,p)$, $E(k) = p(N-1)$ being the average. Since the recovery rate of the network independent from the contact structure, we set it to be equal to γ in (1).

B. Input and Output Maps

To connect the controller proposed above to the network structure we need to introduce to maps, as shown in Fig. 1. The output map extract s and $\imath$ from the full state of the network by counting the number of susceptible and infected subjects, and normalizing it for the total population N. The input map instead provides expressions for the control input on the network level β_{n} given the output of the controller $\beta(s,\imath)$. To this end, we manipulate the first equation of (1) as follows

$$i = \beta\imath s - \gamma\imath \Rightarrow Ni = \beta N\imath s - \gamma N\imath \Rightarrow \dot{I} = \beta I\frac{S}{N} - \gamma I.$$

The term $\beta I\frac{S}{N}$ represents the total infectious pressure on the ode model, i.e. the rate at which infections happen. Assuring that this quantity is preserved between the two models is crucial, as it drives the whole infection process. However, on

the network, the infectious pressure is given by β_{n} times the number of links between infected nodes and susceptible ($S-I$ links), which is a random variable that depends on which individual nodes are infected/recovered and on the topology of the network. To overcome this issue, we introduce the so-called mean-field approximation [7]: on average an infected node is connected to $E[k]$ neighbours, of which we assume that a proportion $\frac{S}{N}$ is susceptible; hence, we set the number of $S-I$ links as $I\frac{S}{N}E[k]$. This allows us to derive an expression for β_{n} as a function of β:

$$\beta_{\mathrm{n}} I(t) E[k] \frac{S(t)}{N} = \frac{\beta}{N} I(t) S(t) \Rightarrow \beta_{\mathrm{n}} = \frac{\beta}{E[k]}. \quad (14)$$

The mean-field approach can be also seen as an approximation where, at any given time, we consider infected nodes as placed on the network uniformly at random.

V. Validation

A. The Codogno case of study

Codogno has been the first city in Lombardy with a diagnosed case of Covid-19, on February, 14 2020. We therefore take it as a prototypical example where to apply our controller. We set $\gamma = \frac{1}{9}\frac{1}{\mathrm{days}}$, in line with 9 days recovery time from symptoms to first negative RT-PCR results, as reported by [25]. We also set $\beta = \frac{R_0}{\gamma}\frac{1}{\mathrm{days}}$ with $R_0 = 2.2$ in line with [26]. Codogno has around $N = 16000$ inhabitants and its hospital had 4 available ICU beds at the time when the pandemics started. Combining WHO guidelines [27] with [28], we assume that at anytime 1% of the infected are in need of intensive care units. The reference policy $\bar{\beta}$ is therefore set to be the one that at its peak saturates the available capacity of the hospital - i.e. $\imath_{\mathrm{th}} = 4/(N2.5)$. The average number of daily contacts at risk in Italy is estimated in [29] to be around 19. We use this as the average degree $E[k]$ of a Erdős-Rényi network to represent the social contact structure of people in Codogno. We consider a time window of 180 days, with an initial condition for the simulation of $I(0) = 800$ of the population, the rest being susceptible. This models the delay in recognizing the presence of an outbreak.

On top of the uncertainties already introduced by the network itself, we consider three levels of further real-world non-ideal behaviors. Level (i) has no further changes. Level (ii) has a delay in the knowledge of the state equal to 2 days, the change of control action happens only at the beginning of each day, the control action is quantized into a reduced set of possible levels $\beta \in \{0, 0.1, \ldots, 0.9, 1\}\beta_{\max}$, and a Gaussian measurement noise with variance 10^{-3} is added. Level (iii) increases the delay to 3 days, the quantization levels reduce in number $\beta \in \{0, 0.2, 0.4, 0.6, 0.8, 1\}\beta_{\max}$, and the noise increases to 0.01 (i.e. about 50% of the actual signal). Note that the delay in the measurements is consistent with the amount of time necessary to collect the results of daily CoVid-19 swab tests and to perform statistical analysis on aggregate statistics to get an estimate of the prevalence. The time discretization models the impossibility of continuously changing policies. The quantization models the presence of a reduced set of Social Distancing Levels which could more easily implemented in the practice than a continuous action. Finally, the noise on data represents the uncertainty to get a precise estimate of the true prevalence from daily tests.

Figs. 4 and 5 show the evolution of infected and of prescribed social distancing respectively. Together with the result when using the proposed feedback action $\beta(s, \imath)$ - we report as comparison the evolution of the uncontrolled epidemics ($\beta = \beta_{\max}$) and the evaluations of the open loop action. Susceptible percentage s are not shown for the sake of space, since in the practice it is not the core goal of our controller to regulate them. All the simulations are repeated 100 times. Every time a new network is generated. Average behaviors are shown as dashed lines, together with the corresponding $\sigma-$band as a translucent area of the same color. In all these cases the controller starts by imposing a period of harsh lock down which lasts a few weeks, after which it moves to values close to the optimal nominal level $\bar{\beta}$. Fig. 6 reports some representative examples of realization.

B. Extensive simulations

We perform extensive simulations for various choices of system parameters. We consider a population of $N = 10^3$ with $\imath(0) = 0.01$, and all possible combinations of $E[k] \in \{4, 8, \ldots, 20\}$, $\gamma \in \{0.06, 0.07, \ldots, 0.14\}\frac{1}{\mathrm{days}}$, and $(\imath(0), \imath_{\mathrm{th}}) \in \{(0.05, 0.04), (0.02, 0.04), (0.02, 0.08)\}$. As for the Codogno validation, each simulation is repeated 100 times, always randomly re-generating the interconnection network. We cannot report here the complete results of our simulations, for the sake of space. We report instead some relevant performance index. The use of the controller consistently induces an reduction of over 99% of the amount of people infected when $\imath > \imath_{\mathrm{th}}$. This is obtained by flattening the infections curve, and as a consequence the total duration of the outbreak doubles. The average level of lock-down imposed is instead more various, depending on the parameters. More specifically, the average value of β increases with $E[k]$ and decreases with an increasing in γ - from a minimum of $0.17\beta_{\max}$ to a maximum of $0.95\beta_{\max}$. In none of the simulations the controller presented critical failures or unstable behaviors.

VI. Discussions and Conclusions

This work preliminary showed that a simple feedback action can dramatically improve the robustness and the effectiveness of an optimal policy for epidemic control. A relevant ourcome observed in all our simulations is that, when control acts on an outbreak that has already reached a significant proportion of the population, the advisable strategy is going into full lockdown until the epidemic curve is brought to acceptable levels, and then gradually relax control measures to keep the epidemic on a sustainable curve. Ideally, when implementing control policies based on serosurveillance data, policy makers have access to the exact state of the system. Clearly, this is not the case. At the very best, daily tests on a fraction of the population can be considered a (noisy) proxy of the state, and robust statistical analysis needs to be carried out to get an estimate of it. Together with several further uncertainties, we tested how the controller behaves when the input data are not exact, but instead normally distributed around the true value. We

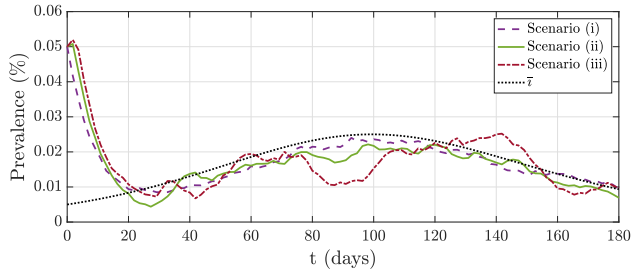

(a) Infected $\imath$

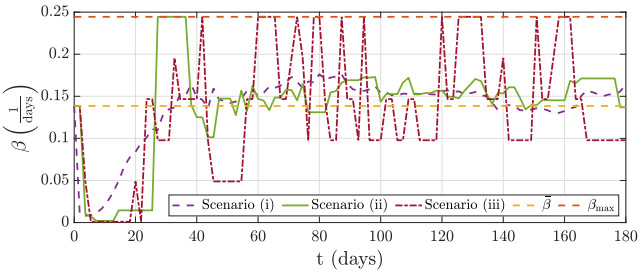

(b) Level of social distancing

Fig. 6. Representative examples of execution for the Codogno case of study, one for each of the three scenarios. Susceptibles are not shown for the sake of space.

observe that the controller can maintain almost equal average performance, while increasing the spreading of the actual realizations. This is however far from being the ultimate solution to model based reactive quarantine design. On the contrary, we see that as a mere first step. Future work will be devoted to investigate the use of more complex model for control design, together with on-line adaptation and learning strategies making the use of these models feasible without the need of a practically unfeasible identification.

REFERENCES

[1] A. B. Gumel, S. Ruan, T. Day, J. Watmough, F. Brauer, P. Van den Driessche, D. Gabrielson, C. Bowman, M. E. Alexander, S. Ardal, *et al.*, "Modelling strategies for controlling sars outbreaks," *Proceedings of the Royal Society of London. Series B: Biological Sciences*, vol. 271, no. 1554, pp. 2223–2232, 2004.

[2] C. J. E. Metcalf, D. H. Morris, and S. W. Park, "Mathematical models to guide pandemic response," *Science*, vol. 369, no. 6502, pp. 368–369, 2020.

[3] A. Goolsbee and C. Syverson, "Fear, lockdown, and diversion: comparing drivers of pandemic economic decline 2020," tech. rep., National Bureau of Economic Research, 2020.

[4] A. I. Bhuiyan, N. Sakib, A. H. Pakpour, M. D. Griffiths, and M. A. Mamun, "Covid-19-related suicides in bangladesh due to lockdown and economic factors: case study evidence from media reports," *International Journal of Mental Health and Addiction*, 2020.

[5] G. Stewart, K. van Heusden, and G. A. Dumont, "How control theory can help us control covid-19," *IEEE Spectrum, 2020. [Online]. Available: https://spectrum.ieee.org/biomedical/diagnostics/ how-control-theory-can-help-control-covid19*.

[6] W. O. Kermack and A. G. McKendrick, "A contribution to the mathematical theory of epidemics," *Proceedings of the royal society of london. Series A, Containing papers of a mathematical and physical character*, vol. 115, no. 772, pp. 700–721, 1927.

[7] I. Z. Kiss, J. C. Miller, and P. L. Simon, *Mathematics of Epidemics on Networks: from exact to approximate models*. Springer, 2017.

[8] A. Vespignani, H. Tian, C. Dye, J. O. Lloyd-Smith, R. M. Eggo, M. Shrestha, S. V. Scarpino, B. Gutierrez, M. U. Kraemer, J. Wu, K. Leung, and G. M. Leung, "Modelling COVID-19," jun 2020.

[9] M. U. Kraemer, C. H. Yang, B. Gutierrez, C. H. Wu, B. Klein, D. M. Pigott, L. du Plessis, N. R. Faria, R. Li, W. P. Hanage, J. S. Brownstein, M. Layan, A. Vespignani, H. Tian, C. Dye, O. G. Pybus, and S. V. Scarpino, "The effect of human mobility and control measures on the COVID-19 epidemic in China," *Science*, vol. 368, pp. 493–497, may 2020.

[10] F. Di Lauro, I. Z. Kiss, and J. Miller, "The timing of one-shot interventions for epidemic control," *medRxiv*, 2020.

[11] R. Djidjou-Demasse, Y. Michalakis, M. Choisy, M. T. Sofonea, and S. Alizon, "Optimal covid-19 epidemic control until vaccine deployment," *medRxiv*, 2020.

[12] D. H. Morris, F. W. Rossine, J. B. Plotkin, and S. A. Levin, "Optimal, near-optimal, and robust epidemic control," *arXiv preprint arXiv:2004.02209*, 2020.

[13] L. Hébert-Dufresne, B. M. Althouse, S. V. Scarpino, and A. Allard, "Beyond r0: Heterogeneity in secondary infections and probabilistic epidemic forecasting," *medRxiv*, 2020.

[14] F. Di Lauro, L. Berthouze, M. D. Dorey, J. C. Miller, and I. Z. Kiss, "The impact of network properties and mixing on control measures and disease-induced herd immunity in epidemic models: a mean-field model perspective," *arXiv preprint arXiv:2007.06975*, 2020.

[15] F. Casella, "Can the covid-19 epidemic be controlled on the basis of daily test reports," *arXiv preprint arXiv:2003.06967*, 2020.

[16] G. Giordano, F. Blanchini, R. Bruno, P. Colaneri, A. Di Filippo, A. Di Matteo, and M. Colaneri, "Modelling the covid-19 epidemic and implementation of population-wide interventions in italy," *Nature Medicine*, pp. 1–6, 2020.

[17] M. M. Morato, I. M. Pataro, M. V. da Costa, and J. E. Normey-Rico, "A parametrized nonlinear predictive control strategy for relaxing covid-19 social distancing measures in brazil," *arXiv preprint arXiv:2007.09686*, 2020.

[18] J. Köhler, L. Schwenkel, A. Koch, J. Berberich, P. Pauli, and F. Allgöwer, "Robust and optimal predictive control of the covid-19 outbreak," *arXiv preprint arXiv:2005.03580*, 2020.

[19] M. Bin, P. Cheung, E. Crisostomi, P. Ferraro, C. Myant, T. Parisini, and R. Shorten, "On fast multi-shot epidemic interventions for post lock-down mitigation: Implications for simple covid-19 models," *arXiv preprint arXiv:2003.09930*, 2020.

[20] R. M. Corless, G. H. Gonnet, D. E. Hare, D. J. Jeffrey, and D. E. Knuth, "On the lambertw function," *Advances in Computational mathematics*, vol. 5, no. 1, pp. 329–359, 1996.

[21] N. S. Barlow and S. J. Weinstein, "Accurate closed-form solution of the sir epidemic model," *Physica D: Nonlinear Phenomena*, p. 132540, 2020.

[22] D. Calzolari, C. Della Santina, and A. Albu-Schäffer, "Exponential convergence rates of nonlinear mechanical systems: The 1-dof case with configuration-dependent inertia," *IEEE Control Systems Letters*, vol. 5, no. 2, pp. 445–450, 2020.

[23] D. T. Gillespie, "Exact stochastic simulation of coupled chemical reactions," *The Journal of Physical Chemistry*, vol. 81, no. 25, pp. 2340–2361, 1977.

[24] B. Bollobás, *Random Graphs*. Cambridge Studies in Advanced Mathematics, Cambridge University Press, 2 ed., 2001.

[25] Y. Ling, S. Xu, Y. Lin, D. Tian, Z. Q. Zhu, *et al.*, "Persistence and clearance of viral RNA in 2019 novel coronavirus disease rehabilitation patients," *Chinese medical journal*, vol. 133, pp. 1039–1043, may 2020.

[26] S. Sanche, Y. Lin, C. Xu, E. Romero-Severson, N. Hengartner, and R. Ke, "RESEARCH High Contagiousness and Rapid Spread of Severe Acute Respiratory Syndrome Coronavirus 2," *Emerging Infectious Diseases*, vol. 26, pp. 1470–1477, jul 2020.

[27] World Health Organisation, "Media statement: Knowing the risks for covid-19," 2020. https://www.who.int/indonesia/news/detail/08-03-2020-knowing-the-risk-for-covid-19, Last accessed on 2020-08-06.

[28] G. Grasselli, A. Pesenti, and M. Cecconi, "Critical Care Utilization for the COVID-19 Outbreak in Lombardy, Italy: Early Experience and Forecast During an Emergency Response," *JAMA*, vol. 323, pp. 1545–1546, 04 2020.

[29] A. Melegaro, M. Jit, N. Gay, E. Zagheni, and W. J. Edmunds, "What types of contacts are important for the spread of infections? using contact survey data to explore european mixing patterns," *Epidemics*, vol. 3, no. 3, pp. 143 – 151, 2011.